1967ZA....67..193U

Zeitschrift für Astrophysik 67, 193—218 (1967)

The Structure of the Outer Atmosphere of the Sun and of Cool Stars

Peter Ulmschneider

Received May 2, 1967

Models of the transition layer and lower corona of the sun and stars of type K1 III, G3 III and G7 V are computed using an improved shock dissipation theory and taking into account the detailed energy balance of shock dissipation and conduction versus flow energy and radiative losses. In the transition layer very steep temperature gradients are obtained since conduction has to balance radiative losses. Comparison with observations yields good agreement.

General conclusions concerning coronal temperatures, temperature gradients, radiative and mass fluxes of cool stars are presented.

Modelle der Übergangsschicht und unteren Korona der Sonne und von Sternen des Typs K1 III, G3 III und G7 V werden berechnet, wobei eine verbesserte Stoßdissipationstheorie benutzt wurde, die das detaillierte Energiegleichgewicht von Stoßdissipation, Wärmeleitung gegen Sonnenwind- und Abstrahlungsverluste berücksichtigt. In der Übergangsschicht ergeben sich sehr steile Temperaturgradienten, da Wärmeleitung die Abstrahlungsverluste ausgleichen muß. Der Vergleich mit den Beobachtungen gibt gute Übereinstimmung. Allgemeine Schlüsse bezüglich Koronatemperaturen, Temperaturgradienten, Strahlungs- und Massenströme von kühlen Sternen werden angegeben.

I. Introduction

In recent years there have been several attempts to construct a more detailed model of the outer atmosphere of stars overlying the photosphere (Allen, 1965; Bird, 1965; Kuperus, 1965; Kanno-Tominaga, 1964; Osterbrock, 1961; Weymann, 1960). This is done usually with severe restrictions as to magnetic fields, the detailed shock structure, the statistical behaviour of the shock production and the uncertainties of the radiative cooling of gas elements in these regions.

We believe however, that in spite of these restrictions which are due to the present lack of observations and theoretical investigations, a general and improved picture of these tenuous regions can be obtained.

The following model seems to be a good working approximation. We consider the magnetic fields to be directed primarily radial such that the gas flow is parallel to the magnetic field lines. This is certainly not good in highly active regions but should not distort the results significantly

© Springer-Verlag • Provided by the NASA Astrophysics Data System

1967ZA.....67..193U

elsewhere. The gas flow is thus uncoupled from the magnetic problem and no energy is fed into magnetohydrodynamic waves. We have then a steady, one-dimensional, spherical gas flow governed by the three equations of continuity, momentum and entropy conservation. The turbulent convection zone produces a wide band of sound and gravity waves which propagate on top of the gas flow. As the maximum of the frequency band of these waves is considerably above the band of no propagation which separates gravity waves from sound waves, the main contribution will be sound waves and not gravity waves (Whitaker, 1963). After some distance, sound waves develop into shocks. The shock wave is here treated as a shell-type discontinuity superposed on the steady gas flow and is governed by the shock equation which describes the behaviour of the strength of the shock wave in the atmosphere.

In our approach we neglected the detailed shock structure, and the statistical nature of shock production, reflection and superposition: the shock structure with its non-equilibrium behaviour is very little understood and the non-statistical approach is warranted in the context of a general model. It has to be noted that the shock equation is necessary here and can not be derived from the previous three equations because of the simplified treatment of the shock structure. The energies dissipated by the shock, and radiated out by the gas element, are treated as source and sink terms in the equation of entropy conservation.

Thus the problem can be described by four time-independent equations of which the equation of continuity can be integrated immediately. Using the integrated form of the entropy equation, the problem is further reduced to three ordinary first-order differential equations which can be integrated with standard numerical methods.

In the regions of the upper photosphere where the shock has not yet formed we use the models of Böhm-Vitense, 1958. The amount of aerodynamical sound produced in the convection zones can be computed from these models, and thus the height at which the shock forms. It was necessary to take into account viscosity at least roughly following the work of Schirmer, 1950, as otherwise shocks would form in regions too dense to be in agreement with observations. This introduces a certain amount of arbitrariness. More arises from the very incomplete knowledge of the growth of the profile behind the shock front. The principle of "shape similarity invariance" (Brinkley-Kirkwood, 1947), which states that the general shape of the shock remains constant during propagation cannot be applied without modification in our strongly varying atmosphere. But this difficulty can be circumvented by postulating complete shock dissipation. This means that when the shock vanishes, all the energy which has been put into it at its formation must have reappeared as dissipated energy.

© Springer-Verlag • Provided by the NASA Astrophysics Data System

1967ZA.....67..193U

II. Thermal and radiative properties of the gas

Before we derive the basic hydrodynamic equations we discuss the thermal and radiative properties of the gas.

1. The thermal properties

The thermal properties are determined by the degree of ionization of the gas. At low altitudes collisional and radiative ionization are balanced term by term by collistional and radiative recombination such that local thermal equilibrium (LTE) exists. At large altitudes, however, the coronal character of the gas predominates, i.e. collisional ionization is balanced by radiative recombination. The so-called corona formula ELWERT, 1952, determines the degree of ionization. In the regions between these two extreme cases the radiation field is of utmost importance and a continuous transition exists between the LTE case and the extreme corona-like case. The ionization in this transition layer depends strongly on the radiation field which is produced in layers far above and below the region where the ionization occurs. The ionization is therefore not dependent on the local properties alone, as in the two extreme cases, but depends on the detailed structure of the whole region. However, in our problem the point of shock formation lies in a relatively large altitude that the corona-like computation of the ionization ratio seems to be a reasonable approximation.

Using the ten most abundant elements (ALLER, 1963), atomic parameters as given by ALLEN, 1964), and the transition rates compiled by HOUSE, 1964, the ratio of specific heats γ, the mean molecular weight μ and the enthalpy per gram H can be computed:

$$\gamma = \frac{\frac{5}{2}(1+\bar{x}) + T\left\{\sum_i \nu_i \sum_{r=1}^{f_i}\left(r\cdot\frac{5}{2} + \left(\sum_{l=1}^{r}\chi_{il}\right)\Big/kT\right)\frac{dx_{ir}}{dT}\right\}}{\frac{3}{2}(1+\bar{x}) + T\left\{\sum_i \nu_i \sum_{r=1}^{f_i}\left(r\cdot\frac{5}{2} + \left(\sum_{l=1}^{r}\chi_{il}\right)\Big/kT\right)\frac{dx_{ir}}{dT}\right\}} \tag{2.1}$$

$$\mu = \frac{\mu_0}{1+\bar{x}} \tag{2.2}$$

$$H = \left\{\frac{5}{2}kT(1+\bar{x}) + \sum_i \nu_i \sum_{r=1}^{f_i} x_{ir} \sum_{l=1}^{r}\chi_{il}\right\}\Big/\mu_0 m_H \tag{2.3}$$

$$\bar{x} = \sum_i \nu_i \sum_{r=1}^{f_i} r\, x_{ir} \tag{2.4}$$

$$\mu_0 = \sum_i \mu_i \nu_i \tag{2.5}$$

where ν_i, f_i, x_{ir}, χ_{ir} are the relative abundance by number, the number of the stages of ionization, the fraction of the element i in the r^{th} ionization stage, the ionization potential of the r^{th} stage of the element i, respectively.

© Springer-Verlag • Provided by the NASA Astrophysics Data System

1967ZA.....67..193U

T is the kinetic temperature, k the Boltzmann constant, m_H the mass of the hydrogen atom, and μ_i the molecular weights.

The partition functions where departures from LTE would come in have been neglected although a calculation showed that bound state energies can become important in a nearly coronalike gas. However, it was found subsequently that this effect did influence the models very little.

The numerical results are shown in Fig. 1.

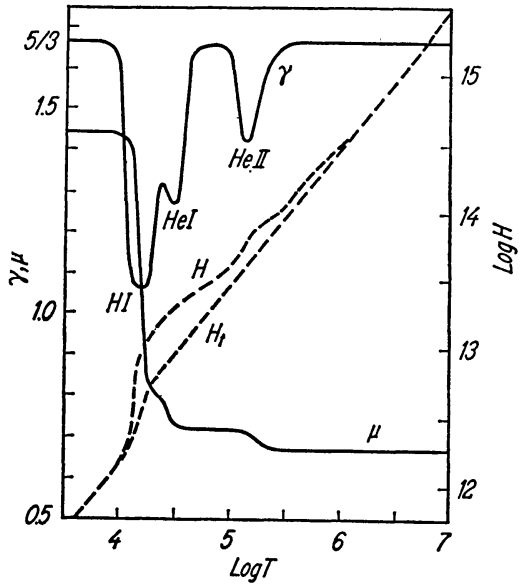

Fig. 1. Ratio of specific heats γ, mean molecular weight μ and enthalpy H per gram as function of temperature T. H_t is the translatory part of the enthalpy only

2. *Radiative losses*

As the amount and distribution of radiative losses in the transition zone between upper photosphere and corona is subject to a rather large margin of error, we consider two cases, a "strong" and a "weak" case, and settle for a "medium" case in the actual computations.

a) Temperatures below 7000° K

The region above the photosphere at these temperatures is optically thin for wave lengths above the Lyman limit, emitting mostly subordinate H continua and the H^- continuum, while the Lyman and Balmer lines are optically thick. For this region we treat the hydrogen continua in LTE.

Weak Case. Noting weak metal lines can be approximately accounted for by multiplying the hydrogen contribution by a factor of 2 (RAJU, 1966) we can estimate the radiation loss using the equilibrium emission

© Springer-Verlag • Provided by the NASA Astrophysics Data System

1967ZA.....67..193U

with the Rosseland mean absorption coefficient:

$$4\pi\,\varepsilon = 4\bar{\varkappa}\,\sigma T^4. \tag{2.6}$$

The actual values do, of course, not have a contribution of scattering. The numerical values were computed from tables given by OSTER, 1957, 1966.

Strong case. An alternate procedure has been suggested by WEYMANN, 1960, (strong case), based on calculations by SEATON, 1955, for cool interstellar gas. In this calculation all continua and resonance lines are treated as optically thin. The ionization is calculated in the coronal approximation. This case predicts much higher radiation losses because of the contribution by (optically thin) resonance lines. We considered this "strong" case as an upper limit. Where the LTE calculations exceed this upper limit they were cut off.

b) Temperatures exceeding 7000° K

Weak case. Here we adopted WEYMANN's, 1960, weak case that includes only the bound-free continua of H and He in addition to bremsstrahlung. Such a spectrum can be considered as a lower limit.

Strong case. Here DOHERTY and MENZEL's, 1965, computation was taken as an upper limit as it exceeded other estimates such as POTTASCH's, 1965, and RAJU's, 1966.

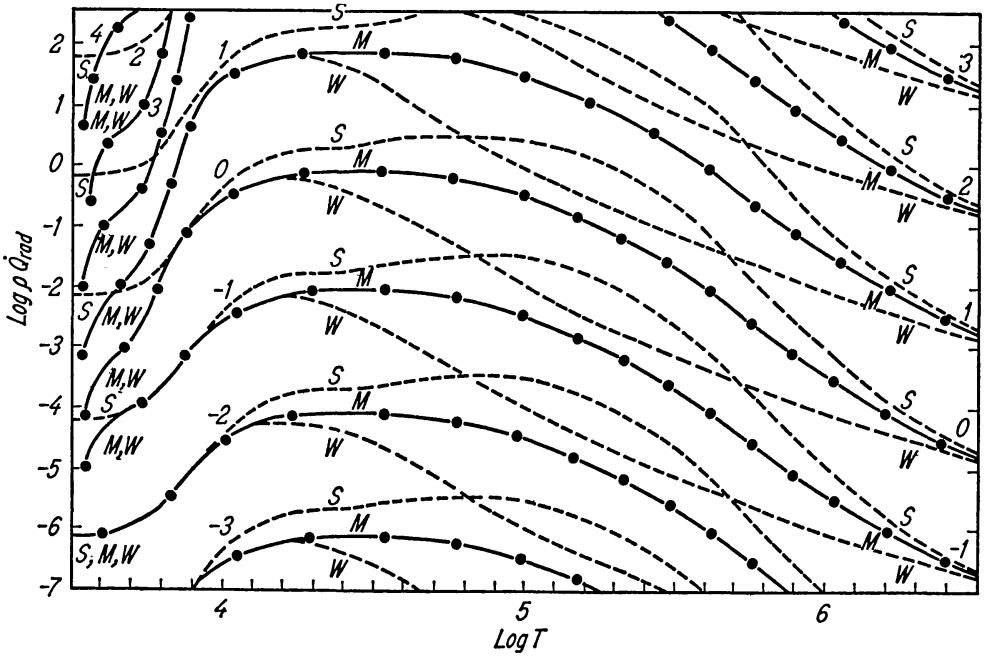

Fig. 2. Radiative loss $\varrho\,\dot{Q}_{\mathrm{RAD}}$ in erg/cm³sec as function of temperature T with gas pressure (Log$p$) as parameter. S strong case, W weak case, M adopted case

© Springer-Verlag • Provided by the NASA Astrophysics Data System

1967ZA.....67..193U

c) Adopted loss function

For temperatures below 7000° K we use the LTE values as discussed under 1). These values may still be somewhat too high as departures from equilibrium keep the ground state overpopulated thus reducing Balmer and Paschen-continua.

For temperatures exceeding 7000° K we divided DOHERTY and MENZEL's values by 5 to 10 to account for the optical thickness of resonance lines. In the very hot regions our adopted curve goes over into the strong case.

The following Fig. 2 gives the energy loss $\varrho\, \dot{Q}_{\mathrm{RAD}}$ adopted (labeled M) in erg/cm³sec as function of temperature with the logarithm of the gas pressure as parameter. The curves labled S and W are the "strong" and "weak" cases.

III. The basic equations

We now review the basic equations for our problem.

1. Hydrodynamic equations

The steady flow of non-viscous gas streaming with velocity $\vec{u}$ can be described by there equations of

Continuity: $$\nabla \cdot \varrho\, \vec{u} = 0\,. \tag{3.1}$$

Motion: $$(\vec{u} \cdot \nabla)\, \vec{u} = -\frac{1}{\varrho} \nabla p - g\, \vec{x}\,. \tag{3.2}$$

Entropy: $$\vec{u} \cdot \nabla S = \dot{S}_{\mathrm{ext}}\,. \tag{3.3}$$

These equations and the equation of state, $S = S(p, \varrho)$ (entropy) determine the five functions $\vec{u}\,(x)$, $\varrho\,(x)$ density), $p(x)$ (pressure) uniquely, if we specify the respective boundary conditions and if the external entropy influx $\dot{S}_{\mathrm{ext}}$ is a given function of $\vec{u}$, ϱ and p. The additional shock equation and our estimate about radiative losses (Sec. IIb) will give us this necessary $\dot{S}_{\mathrm{ext}}$. In (3.2) g is the gravitational acceleration, $\vec{x}$ a unit vector in outward radial direction.

2. Pressure and flow equations

In our spherical one-dimensional geometry with radial distance x it is convenient to use a dimensionless variable,

$$r = \frac{x}{r_0}\,, \tag{3.4}$$

where r_0 is a reference level for which we take $\bar{\tau} = .003$ for the sun, and $\bar{\tau} = .01$ for the other stars. The flow Mach number is defined by

$$M = \frac{|\vec{u}|}{c}\,, \tag{3.5}$$

© Springer-Verlag • Provided by the NASA Astrophysics Data System

1967ZA.....67..193U

where

$$c^2 = \gamma \frac{p}{\varrho} = \gamma \frac{RT}{\mu} . \tag{3.6}$$[1]

c is the sound velocity, T the kinetic temperature, R the gas constant, γ and μ were previously defined. Integrating (3.1) over a conical section we find the pressure equation

$$p = \frac{p_0 \mu_0 M_0 c_0}{T_0} \frac{T}{\mu M c r^2} , \tag{3.7}$$

where the subscript zero indicates values at the reference level $r = 1$. Using (3.1) and (3.2), the flow equation reads

$$\frac{dM}{dr} = \frac{M}{1 - \gamma M^2} \left(\frac{1 + \gamma M^2}{2 c^2} \frac{dc^2}{dr} - \frac{1}{\gamma} \frac{d\gamma}{dr} + \frac{\gamma g_0 r_0}{c^2 r^2} - \frac{2}{r} \right) . \tag{3.8}$$

This equation has been given by BIRD, 1964, except for the term $\sim \frac{d\gamma}{dr}$; c.f. also CHAPMAN, 1954; LÜST, 1962; PARKER, 1963.

3. The shock equation

The shocks we have to deal with develop out of sound wave trains of different length and frequencies due to the production in a turbulent convection zone. For simplicity we consider monochromatic sound waves of frequency ν_0 for which we take the maximum frequency of the frequency spectrum (OSTERBROCK, 1961). Different kinds of shock shapes can develop from sound waves. What shape eventually develops can only be specified by a detailed growth calculation for sound waves, taking into account viscosity, radiative losses as well as conduction and the non-equilibrium structure of the shock front (SKALAFURIS, 1965). However, a simplified approach seems to be useful, because we are not interested in the shock as a time dependent entity, but as a means to deposit over long time averages a certain amount of energy in a specified volume of gas. Therefore we feel that the simplified model of a shock will still give a reliable picture.

The model of the shock which we assume is the simple discontinuity behind which the state variables relax to the state present before the shock arrived. This so called profile of the shock may be triangular, sawtooth, exponential, bell-shaped, etc.

Let us define the shock Mach number M_s,

$$M_s = \frac{U - u_1}{c_1} , \tag{3.9}$$

where from now on the subscript 1 indicates the variables of the undisturb-

[1] Actually $c^2 = \left(\frac{\partial p}{\partial \varrho}\right)_s = \left(\gamma - \frac{(\gamma - 1) T}{\mu} \frac{d\mu}{dT}\right) \frac{p}{\varrho}$ but the second term in the bracket is at most about 6% of the first term and can therefore be neglected.

© Springer-Verlag • Provided by the NASA Astrophysics Data System

1967ZA.....67..193U

ed gas in front of the shock, while 2 indicates the value directly after passage of the discontinuity. U is the velocity of the shock, while u_1 is the gas velocity and c_1 the sound velocity in front of the shock.

It can be shown (LANDAU-LIFSHITZ, 1959) that we then have

$$\frac{p_2}{p_1} = \frac{2\,\gamma\,M_s^2 - (\gamma - 1)}{\gamma + 1} \equiv \phi\,, \tag{3.10}$$

$$\frac{\varrho_2}{\varrho_1} = \frac{u_1}{u_2} = \frac{(\gamma + 1)\,M_s^2}{(\gamma - 1)\,M_s^2 + 2} \equiv \theta\,, \tag{3.11}$$

$$\frac{c_2}{c_1} = \left(\frac{\phi}{\theta}\right)^{1/2} \equiv \zeta\,, \tag{3.12}$$

$$\frac{u_2}{c_1} = \xi + M\,, \tag{3.13}$$

with

$$\xi \equiv \frac{2\,M_s^2 - 2}{(\gamma + 1)\,M_s}\,, \tag{3.14}$$

where γ is now a function of the kinetic temperature T.

From the work of SCHIRMER, 1950, we estimate what shape the shock profile will have. If the sound wave carries a large amount of energy, while no viscosity and radiation losses are considered, it grows very fast and develops into a shock in a high-density area and a sawtooth shock develops with small ($M_s \approx 1$). However, if, as Schirmer has shown, the growth is strongly inhibited by the medium, the sound wave will travel into areas of much lower density and a strong triangular shock will finally develop ($M_s \gg 1$). The shock equation should therefore not depend on the smallness of M_s but should be valid for small as well as large values of M_s.

When our calculations were performed, three different shock equations, which describe the behaviour of M_s during the passage of the shock through a medium, were common in the literature:

1. The approach developed by BRINKLEY and KIRKWOOD, 1947, for underwater and atomic explosions. Here, a shock of *arbitrary strength* is considered, and use is made of the "principle of shape similarity invariance" which is based essentially on experimental results. This approach has been applied by SCHATZMANN, 1949; WEYMANN, 1960 and OSTERBROCK, 1961, to the solar atmosphere for *small* shock Mach numbers.

2. The approach treating shocks as the result of the development of large amplitude sound waves which has been given by LANDAU and LIFSHITZ, 1959. This approach was adopted by KUPERUS, 1965, to stellar coronas, again for *small* shock Mach numbers.

3. The approach based on the theory for shock tube experiments that was developed by WHITHAM, 1959, and BIRD, 1961, 1964, 1965, and adopted by BIRD to the solar atmosphere for *arbitrary* shock Mach numbers.

© Springer-Verlag • Provided by the NASA Astrophysics Data System

1967ZA.....67..193U

We shall follow BIRD's treatment but include variability of γ and a dissipation term on the shock Mach number M_s as suggested by methods 1 and 2. The variability of γ can simply be included (ULMSCHNEIDER, 1966) in the derivation of BIRD's shock equation. This will give eq. (3.21) except for the last term $\sim \chi$. In a plane atmosphere $\left(\frac{2}{r} \to 0\right)$ with $\gamma = \text{const.}$, no gravity $(g_0 \to 0)$ and no temperature gradient $\left(\frac{dc^2}{dr} \to 0\right)$ we find with this equation $\frac{dM_s}{dr} = 0$. This indeed is correct for shock-tube calculations where the energy is supplied by the moving piston, and the shock has an infinite rectangular shape. In our case however the energy loss in the gas modifies the strength of the shock as suggested by methods 1 and 2.

After a shock has passed a volume element of gas the internal energy has increased and, although the pressure has come back to its equilibrium value p_1, the volume has increased. Thus, the total work ΔW done is

$$\Delta W = \Delta E + p_1 \Delta V = \Delta H \,. \tag{3.15}$$

Here, H is again the enthalpy per gram. If $D(x)$ is the total energy of the shock per unit area of initial surface in spherical geometry, then

$$\frac{dD(x)}{dx} = -\varrho_1 \Delta H \frac{x^2}{r_0^2} \,. \tag{3.16}$$

Considerations of thermodynamics show that

$$\Delta H = T_1 \Delta S = T_1 c_v \ln\left\{\frac{p_2}{p_1}\left(\frac{\varrho_2}{\varrho_1}\right)^{-\gamma}\right\} = \frac{c_0^2}{\gamma(\gamma-1)} \cdot \ln(\phi\, \theta^{-\gamma}) \,. \tag{3.17}$$

Hence, the energy of the shock is:

$$D(x) = \frac{x^2}{r_0^2} \int_{t_x}^{\infty} (p - p_1)\, u\, dt \,. \tag{3.18}$$

Here pressure p and velocity u refer to the shock profile, t_x is the time of the arrival of the shock at point x. Using the "principle of similarity invariance" BRINKLEY-KIRKWOOD, 1947, we can write for eq. (3.18):

$$D(x) = \frac{x^2}{r_0^2}(p_2 - p_1)\, u_2\, \tilde{\mu}\, \tilde{\nu} \approx \frac{x^2}{r_0^2}(\phi - 1)\, \xi\, \varrho_1 \frac{c_1^3}{\gamma} \tilde{\mu}\, \tilde{\nu} \,, \tag{3.19}$$

where $\tilde{\mu}\,\tilde{\nu} = \frac{P}{3}$ for triangular and $= \frac{P}{12}$ for sawtooth shocks. Differentiating eq. (3.19) and equating the result to (3.16) we obtain

$$\frac{dM_s}{dx} = -\frac{1}{4\, c_1} \frac{(\gamma+1)^2}{\gamma(\gamma-1)} \frac{\mathrm{Ln}(\phi\, \theta^{-\gamma})}{\left(3\, M_s^2 - 2 - \frac{1}{M_s^2}\right)\left(1 + \frac{M}{M_s}\right)} \tag{3.20}$$

where the flow in front of the shock is included.

© Springer-Verlag • Provided by the NASA Astrophysics Data System

1967ZA.....67..193U

Dropping the subscripts 1 we can finally write for the complete shock equation:

$$\frac{dM_s}{dr} = \frac{\zeta\eta M_s}{1-\gamma M^2}\left\{-\frac{(\xi+2M-(\gamma\xi+2\zeta)M^2}{2}\frac{1}{c^2}\frac{dc^2}{dr}+\right.$$
$$+\frac{1}{\xi+\zeta+M}\left(\zeta(\xi+\zeta)-1+(\zeta-\gamma(\xi+\zeta))M\right)\frac{g_0 r_0}{c^2 r^2}-$$
$$-\frac{1}{\xi+\zeta+M}\left(\zeta\xi-\xi M+(\zeta^2-1-(\gamma-1)\zeta\xi)M^2-\right. \quad (3.21)$$
$$\left.\left.-(\gamma-1)\zeta M^3\right)\frac{2}{r}-(\delta-M+(\zeta-\gamma\delta)M^2)\frac{1}{\gamma}\frac{d\gamma}{dr}\right\}-$$
$$-\frac{1}{4}\frac{\chi r_0}{c\tilde{\mu}\tilde{\nu}\left(1+\frac{M_s}{M}\right)},$$

with ξ, ζ, θ, ϕ defined previously, and

$$\eta \equiv \frac{(\gamma+1)/2}{\frac{2}{\gamma+1}((\gamma-1)M_s^2+2)+\zeta(M_s+M_s^{-1})} \quad (3.22)$$

$$\delta \equiv \frac{\xi}{\gamma+1}\left(\frac{M_s}{\theta\zeta}-\gamma\right), \quad (3.23)$$

$$\chi \equiv \frac{(\gamma+1)^2}{\gamma(\gamma-1)}\frac{\mathrm{Ln}\,(\phi\,\theta^{-\gamma})}{(3M_s^2-2-M_s^{-2})}. \quad (3.24)$$

This equation can be shown to reduce to the three shock equations of methods 1, 2, and 3 in their respective regions of validity.

4. The energy equation

It is now easy to show how from eq. (3.3) the so-called energy equation can be derived.

From eq. (3.3) follows (LANDAU-LIFSHITZ, 1959)

$$-\nabla\cdot\varrho\,\vec{u}\left(\frac{1}{2}u^2+H\right)-\varrho\,\vec{u}\cdot g\,\vec{x}+\varrho\,T\dot{S}_{\mathrm{ext}}=0. \quad (3.25)$$

The irreversible external heat flux consists of mechanical energy deposited by the shock, radiation and conduction:

$$\varrho\,T\dot{S}_{\mathrm{ext}}=\varrho\dot{Q}_{\mathrm{MECH}}-\varrho\dot{Q}_{\mathrm{RAD}}+\varrho\dot{Q}_{\mathrm{COND}}. \quad (3.26)$$

$\varrho\dot{Q}_{\mathrm{RAD}}$ is given in Sec. II 2. With eq. (3.16) and ν_0 shocks per second we have

$$\varrho\dot{Q}_{\mathrm{MECH}}=\nu_0\frac{dD}{dx}=\nu_0\varrho\frac{x^2}{r_0^2}\frac{c^2}{\gamma(\gamma-1)}\ln(\phi\theta^{-\gamma}). \quad (3.27)$$

The well known conduction term is ($K_0 = 6\cdot10^{-7}$erg/cm^2 sec grad$^{5/2}$, PARKER, 1963)

$$\varrho\dot{Q}_{\mathrm{COND}}=\nabla\cdot K_0 T^{5/2}\nabla T. \quad (3.28)$$

© Springer-Verlag • Provided by the NASA Astrophysics Data System

1967ZA.....67..193U

With the aid of eq. (3.1) we can write

$$\varrho \tilde{u} \cdot g \tilde{x} = - \nabla \cdot \varrho \tilde{u} \frac{g_0 r_0^2}{x} , \tag{3.29}$$

and obtain

$$\varrho \dot{Q}_{\mathrm{MECH}} - \varrho \dot{Q}_{\mathrm{RAD}} = \nabla \cdot \left\{ \varrho \tilde{u} \left(\frac{1}{2} u^2 + H - \frac{g_0 r_0^2}{x} \right) - K_0 T^{5/2} \nabla T \right\} . \tag{3.30}$$

Integrating this equation over a spherical zone, using eq. (3.1) again and going over to the dimensionsless variable r, gives finally the energy equation

$$\frac{dT}{dr} = \frac{r_0}{K_0 T^{5/2}} \frac{1}{r^2} \left\{ \mathrm{FLOW} - \mathrm{DISS} + \mathrm{RAD} + \frac{K_0}{r_0} T_0^{5/2} \frac{dT_0}{dr} \right\} . \tag{3.31}$$

The symbolic notations FLOW, DISS, RAD are defined by:

$$\mathrm{RAD} \equiv \int_1^r r_0 \varrho \dot{Q}_{\mathrm{RAD}} r^2 \, dr , \tag{3.32}$$

$$\mathrm{DISS} \equiv \tilde{L} \int_1^r r_0 v_0 p \frac{1}{\gamma - 1} \ln(\theta \phi) \, r^4 \, dr , \tag{3.33}$$

$$\mathrm{FLOW} \equiv \varrho_0 M_0 c_0 \left\{ \left(\frac{1}{2} M^2 c^2 + H - \frac{g_0 r_0}{r} \right) - \left(\frac{1}{2} M_0^2 c_0^2 + H_0 - g_0 r_0 \right) \right\} , \tag{3.34}$$

where the subscript o labels again the variables at references level $r = 1$. $\tilde{L}$ is a multiplication factor which arises from the growth of the shock profile in the atmosphere. Presently we have $\tilde{L} = 1$. Writing

$$\mathrm{COND} \equiv \frac{K_0}{r_0} \left(T^{5/2} \frac{dT}{dr} r^2 - T_0^{5/2} \frac{dT_0}{dr} \right) , \tag{3.35}$$

we obtain the balance relation

$$\mathrm{COND} = \mathrm{FLOW} + \mathrm{RAD} - \mathrm{DISS} \tag{3.36}$$

The physical interpretation of the quantities RAD, DISS, FLOW and COND is that they represent the total energies (per cm^2 of the initial surface) that are radiated, dissipated transformed into stellar wind and conducted, respectively per second within the column bounded by $r = 1$ and $r = r$. From eq. (3.36) we see that the conduction term acts as a reservoir from which we can borrow energy to radiate or increase the thermal and kinetic energy of the stellar wind in case that the shock dissipation is not yet sufficient to compensate for the losses: DISS $<$ (FLOW + RAD). However ultimately the dissipation term must equal the sum of flow and radiation terms, if the energy to drive the stellar wind and to provide for radiation losses comes from within the star and not from an external reservoir. This condition of a "shock dominated solution" is discussed below in detail.

© Springer-Verlag • Provided by the NASA Astrophysics Data System

1967ZA.....67..193U

IV. Boundary conditions and topology of the full set of equations. The principle of complete shock dissipation

The flow equation (3.8), the shock equation (3.21) and the energy equation (3.30) form a complete set of equations for the three unknown functions M, M_s, T respectively. The quantities γ, H, c^2 are functions of T only and the pressure p can be computed with eq. (3.7) as function of T and M. Thus we have a closed system and can perform the integration provided we have the boundary values M_0, M_{s_0}, T_0 and know the values of the constants which enter our various equations.

1. The boundary conditions T_0, p_0, M_{s_0}

To compute boundary conditions we use the models of BÖHM-VITENSE, 1958, which we continue isothermally from $\bar{\tau} = .01$ on. For the sun we use in addition the model of HEINTZE, 1965, for comparison.

a) Noise production

The amount of acoustical noise produced and flowing in the outward direction can be shown (OSTERBROCK, 1961) to be:

$$\pi F^+_{m_0} = \frac{1}{2} \int \frac{38\, \varrho\, \bar{v}^8}{c^5 l}\, dh\,, \tag{4.1}$$

where ϱ is the density, $\bar{v}$ the mean velocity of the turbulent elements, c the sound velocity, l the scale height. Velocity and density profiles were calculated from the BÖHM-VITENSE, 1958, models, and the integration eq. (4.1) performed numerically. The frequency of the sound waves ν_0 has to be above the cut-off frequency ν_c (KUPERUS, 1965)

$$\nu_0 = \frac{\bar{v}}{l} \tag{4.2}$$

$$\nu_c = \frac{\gamma g}{4\pi c} \tag{4.3}$$

b) Height of shock formation

As long as viscous dissipation, radiative and conductive losses are neglected we can write

$$\pi F^+_{m_0} = \varrho\, \tilde{u}^2 c \quad \text{or} \quad \frac{\tilde{u}}{c} = \sqrt{\frac{\pi F^+_{m_0}}{\gamma p c}}\,, \tag{4.4}$$

where $\tilde{u}$ is the perturbation velocity in the sound wave and p the pressure in the atmosphere. Following the hills in the sound profiles till they catch up with the valleys, we find (OSTERBROCK, 1961):

$$\int_{t(H_P)}^{t(H_F)} \tilde{u}\, dt = \frac{\lambda}{4} \text{ or } 4\nu_0 \sqrt{\frac{\pi F^+_{m_0}}{\gamma}} \int_{H_P}^{H_F} (pc)^{-\frac{1}{2}}\, dh = c\,. \tag{4.5}$$

© Springer-Verlag • Provided by the NASA Astrophysics Data System

1967ZA.....67..193U

H_P and H_F are the heights of the production of sound waves and the formation of the shock respectively. Numerically, it turns out that condition (4.5) is within a few percent equal to the much simpler condition

$$\tilde{u} = c \,. \tag{4.6}$$

With eq. (4.4) this leads to

$$p = \frac{\pi F^{+}_{m_0}}{\gamma c} \tag{4.7}$$

Using the boundary temperature T_0 at $\bar{\tau} = .01$ we can compute the pressure p at shock formation and the height H_F.

However, viscosity and radiative losses can be taken into account, at least roughly, from the work of SCHIRMER, 1950. As the growth of the sound waves is opposed, they travel to regions of lower pressure p until they form shocks:

$$p_0 = \frac{p}{\tilde{l}} \tag{4.8}$$

for $\tilde{l}$, the shape compression factor, SCHIRMER found the value of 2.6. Figure 5 shows the influence of this factor $\tilde{l}$. The curve labeled 12 shows a model computation with no viscous and radiative losses ($\tilde{l} = 1$). We adopt here the value $\tilde{l} = 4.9$.

The zero reference level ("radius of the star") has been taken from BÖHM-VITENSE's computations. For stars, this corresponds to $\bar{\tau} = 0.1$, for the sun to the customary $\bar{\tau} = .003$.

c) The initial shock Mach number M_{s_0}

After viscous and radiative losses have opposed the growth of the sound wave, a strong (triangular shapes) shock forms in the tenuous atmosphere. M_s can be found from eq. (3.19):

$$\pi F^{+}_{m_0} = v_0 D = c_0 p_0 \frac{(M^2_{s_0} - 1)^2}{M_{s_0}} \frac{4\gamma}{(\gamma + 1)^2} \cdot \frac{1}{6} \tag{4.9}$$

With eq.'s (4.7), (4.8), (4.9)

$$M_{s_0} = 3.9 \,. \tag{4.10}$$

Results are summarized in Table 2.

2. The initial flow Mach number M_0

The boundary condition for the flow Mach number M_0 has to be treated differently. If we start with arbitrary M_0 we find that for an infinite number of M_0 the solutions become either multivalued (and therefore unphysical) or subsonic (see Fig. 3). These solutions are known as supercritical and subcritical solutions, respectively (PARKER, 1963; LÜST, 1962). In addition, there are three critical values of M_0 for which

© Springer-Verlag • Provided by the NASA Astrophysics Data System

1967ZA.....67..193U

the solutions become supersonic. But supersonic flow has been found to persist for the sun (PARKER, 1965). We assume that this is the case for other stars as well. However, two of the three critical solutions will be excluded on physical grounds.

3. The types of solutions

Due to the more or less independent behaviour of the shock equation (3.21), which provides only the DISS-term to the energy equation (3.31) the types of solutions can be classified simply on the basis of the relative magnitude of the energy term DISS, COND versus RAD, FLOW, and of the known supercritical and subcritical behaviour of the flow equation. Starting with a high value of M_0 (see Fig. 3) we find that FLOW $\gg$ DISS, RAD, and obtain a conduction dominated (CD) solution. It corresponds to a solution where the energy is supplied from infinity through a temperature gradient and conduction. The critical solution "CCD" in this region is therefore excluded on physical grounds.

Lowering M_0 further we find DISS = FLOW + RAD at some point in the atmosphere which means the temperature-gradient becomes zero and the atmosphere shows a shockdominated solution (SD). The energy is supplied from within the star in this case. For the largest M_0 in this region we find DISS > FLOW > RAD and a critical shockdominated solution "CSDF" with the flow-term being the important one.

Lowering M_0 further reduces the importance of FLOW and DISS > RAD > FLOW. This leads to the critical, shock-dominated solution

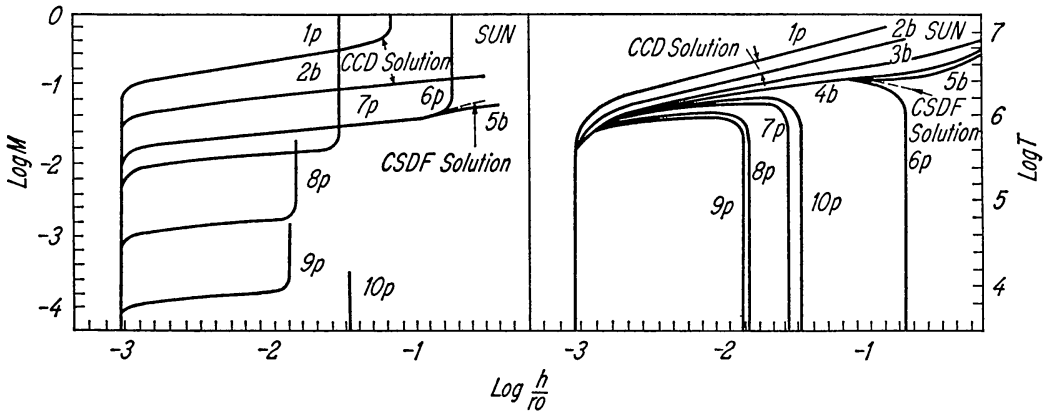

Fig. 3. Iteration to the critical solution. Flow Mach number M (left) and temperature T (right) as function of height h above the solar radius r_0. p labels supercritical, b subcritical solutions. The initial flow Mach number decreases from solution 1 ($M_0 = 5 \cdot 10^{-3}$), 2 ($M_0 = 2 \cdot 10^{-3}$), 3 ($M_0 = 1 \cdot 10^{-3}$), 4 ($M_0 = 7.5 \cdot 10^{-4}$), 5 ($M_0 = 7.22 \cdot 10^{-4}$), 6 ($M_0 = 7.17 \cdot 10^{-4}$), 7 ($M_0 = 4 \cdot 10^{-4}$), 8 ($M_0 = 5 \cdot 10^{-5}$), 9 ($M_0 = 5 \cdot 10^{-6}$), 10 ($M_0 = 1 \cdot 10^{-7}$). For all solutions the multiplication factor $\tilde{L}$ is 6

© Springer-Verlag • Provided by the NASA Astrophysics Data System

1967ZA....67..193U

"CSDR" with radiation as most important term. This solution can be excluded as it provides initial temperature gradients in excess of 5000°/cm. Therefore the CSDF solution seems to be the only reasonable possibility (see Fig. 3).

d) When we performed the integration with the given boundary conditions and with $\tilde{L} = 1$ in the DISS-term (eq. 3.33), we found that when the shocks vanished ($M_s \to 1$) only a few percent of the energy which we put into the shocks at the point of transformation from the sound waves reappeared in the form of dissipation. Detailed investigations were made to find the reason of this obvious contradiction. It was found that the principle of shape similarity invariance which requires $\tilde{\mu}\tilde{\nu} = \text{const}$ does not describe the situation correctly. As a matter of fact, $\tilde{\mu}\tilde{\nu}$ does not remain constant, and the originally triangular shape changes. The correct procedure would be thus to develop a detailed theory of growth of the profile behind the shock similar to the work done by SCHIRMER, 1950, for sound waves.

However, as we are not interested in the exact shape of the shocks but in their nature of providing the necessary energy term DISS to compensate RAD and FLOW we can approximately treat the problem the following way: We multiply DISS with a factor $\tilde{L}$ which increases the dissipation and find the correct factor $\tilde{L}$ by postulating that, when the shocks vanish, all energy originally in the sound waves must be dissipated and reappear as DISS:

$$\text{DISS}_f = \pi F^+_{m_0} . \tag{4.11}$$

As the temperature and flow profiles are not changed very much by varying $\tilde{L}$, (compare Fig. 3 and 4), a relatively unsophisticated iteration to find $\tilde{L}$ (exhibited in Table 1) is sufficient.

Table 1. *Iteration to find the correct factor L for which we have complete shock dissipation. M_e is the initial flow Mach number of the critical solution, $DISS_f$ is the final dissipated flux of shock energy when the shocks have vanished. Values in brackets are extrapolated*

$\tilde{L}$	Sun G2 V		K1 III		G3 III		G7 V	
	M_e	DISS_f	M_e	DISS_f	M_e	DISS_f	M_e	DISS_f
6	$7.15 \cdot 10^{-4}$	$1.08 \cdot 10^{7}$	$1.07 \cdot 10^{-4}$	$7.20 \cdot 10^{6}$	$3.50 \cdot 10^{-4}$	$1.95 \cdot 10^{7}$	$1.40 \cdot 10^{-3}$	$1.20 \cdot 10^{6}$
9	$1.13 \cdot 10^{-3}$	$1.61 \cdot 10^{7}$	$7.47 \cdot 10^{-4}$	$1.36 \cdot 10^{7}$	$6.97 \cdot 10^{-4}$	$2.85 \cdot 10^{7}$	$2.04 \cdot 10^{-3}$	$3.01 \cdot 10^{6}$
10	$1.25 \cdot 10^{-3}$	$1.75 \cdot 10^{7}$	$(9.3 \cdot 10^{-4})$	$(1.60 \cdot 10^{7})$				
11					$(9.2 \cdot 10^{-4})$	$(3.40 \cdot 10^{7})$	$2.45 \cdot 10^{-3}$	$7.00 \cdot 10^{6}$

V. Results

The numerical results of the critical CSDF solutions for our four stellar models are exhibited in Fig. 4, 6, 7, 8 and Tables 2—3. An IBM 7094 computer was used and a 5th order Runge-Kutta-method (ZONNEVIELD, 1964), where the 6th order term was kept to regulate the stepsize.

© Springer-Verlag • Provided by the NASA Astrophysics Data System

1967ZA....67..193U

Table 2. *Initial values and final results of our four stellar models*

		Sun G2 V	K1 III	G3 III	G7 V	
T_{eff}	°K	5800	4400	5000	5000	effective temperature
Log g	$\frac{\text{cm}}{\text{sec}^2}$	4.45	2.50	3.00	4.45	surface gravity
r_0	km	$6.95 \cdot 10^5$	$4.9 \cdot 10^6$	$3.3 \cdot 10^6$	$4.9 \cdot 10^5$	star radius, zero reference level
$\Pi F^+_{m_0}$	$\frac{\text{erg}}{\text{cm}^2\,\text{sec}}$	$1.6 \cdot 10^7$	$1.6 \cdot 10^7$	$3.4 \cdot 10^7$	$3.0 \cdot 10^6$	noise energy flux
ν_0	sec^{-1}	$9.0 \cdot 10^{-3}$	$1.5 \cdot 10^{-4}$	$5.0 \cdot 10^{-4}$	$7.9 \cdot 10^{-3}$	maximum of noise frequency spectrum
ν_c	sec^{-1}	$3.3 \cdot 10^{-3}$	$3.9 \cdot 10^{-5}$	$1.2 \cdot 10^{-4}$	$3.6 \cdot 10^{-3}$	cut-off frequency for sound
$\bar{\tau}\,(H = 0)$		.003	.01	.01	.01	mean opacity at zero height level
H_p	km	−360	−26200	−7150	−260	height of sound generation
H_F	km	643 / 1060	29100	12700	790	height of shock formation* (HEINTZE's model)
T_0	°K	4064	3069	3793	3793	initial temperature
p_0	$\frac{\text{dyn}}{\text{cm}^2}$	3.2	3.67	7.08	.619	initial pressure
Ms_0		3.9	3.9	3.9	3.9	initial shock Mach number
M_0		$1.14 \cdot 10^{-3}$	$9.3 \cdot 10^{-4}$	$9.2 \cdot 10^{-4}$	$2.04 \cdot 10^{-3}$	initial flow Mach number
u_0	$\frac{\text{cm}}{\text{sec}}$	$7.1 \cdot 10^2$	$5.1 \cdot 10^2$	$5.6 \cdot 10^2$	$1.2 \cdot 10^3$	gas velocity at zero reference level
$\varrho_0 u_0 r^2$	$\frac{\text{g}}{\text{cm}^2\,\text{sec}}$	$9.7 \cdot 10^{-9}$	$1.0 \cdot 10^{-8}$	$1.8 \cdot 10^{-8}$	$3.5 \cdot 10^{-9}$	mass flux
ML	$\frac{\text{g}}{\text{sec}}$	$5.9 \cdot 10^{14}$	$3.2 \cdot 10^{16}$	$2.5 \cdot 10^{16}$	$1.1 \cdot 10^{15}$	total mass loss
πF_{RAD}	$\frac{\text{erg}}{\text{cm}^2\,\text{sec}}$	$3.5 \cdot 10^6$	$3.5 \cdot 10^6$	$7.4 \cdot 10^6$	$4.0 \cdot 10^5$	total U-V flux
UVL	$\frac{\text{erg}}{\text{sec}}$	$2.1 \cdot 10^{29}$	$1.1 \cdot 10^{31}$	$1.0 \cdot 10^{31}$	$1.2 \cdot 10^{28}$	total U-V radiation loss
T_{COR}	°K	$3.2 \cdot 10^6$	$2.8 \cdot 10^6$	$3.5 \cdot 10^6$	$1.7 \cdot 10^6$	maximum coronal temperature

* It has been kept in mind that this value depends strongly on the statistical nature of the noise production. Behind large turbulent elements there is a "noise shadow". The reduced noise level will produce shocks at a much greater altitude which gives the gas a chance to cool (spicules). Thus the solar transition layer has the appearance of a "spiked ball".

VI. Discussion of the Solar Results

1. Discussion of the model

As soon as the shock has formed, shock energy is dissipated very rapidly. The energy serves primarily to heat the gas (balance of the

© Springer-Verlag • Provided by the NASA Astrophysics Data System

1967ZA.....67..193U

Table 3. *Temperature rise in the transition layer. The heights given are heights above the level of shock formation*

Temp	Sun km	K1 III km	G3 III km	G7 V km
T_0	0	0	0	0
$7 \cdot 10^3$	.056			
$1 \cdot 10^4$	.062	.02	.01	.017
$2 \cdot 10^4$	.085			
$5 \cdot 10^4$	.25	.23	0.13	.65
$1 \cdot 10^5$	1.15	1.05	.54	4.18
$2 \cdot 10^5$	5.54			
$5 \cdot 10^5$	65.5	54.7	30.1	261
$1 \cdot 10^6$	493	470	253	2350

FLOW-term) while conduction is not yet important:

$$\text{DISS} = \text{FLOW} + \text{RAD} \tag{6.1}$$

The temperature rise will bring the gas quickly into a temperature region where the radiative losses (RAD) increase rapidly by approximately 4 orders of magnitude. The comparatively slow variation of dissipation (DISS) cannot compete with the radiative losses, and the energy must be supplied by conduction (COND). The more energy is radiated out, the steeper the temperature gradient must be in order to balance this radiation by means of conduction:

$$\text{COND} = \text{RAD} + \text{FLOW} \tag{6.2}$$

This behaviour can be illustrated by a comparison with BIRD's, 1965, solar models that balance dissipation against thermal and kinetic energy in the solar wind:

$$\text{DISS} = \text{FLOW} \tag{6.3}$$

Bird finds the same steep initial temperature rise due to the large shock dissipation. However, as conduction is neglected as well as radiative losses, the steepening influence of a large conduction term balancing a large radiation term is not experienced and his model temperatures rise much less steeply further out.

The temperature region of extreme radiative losses is thus passed with a very steep temperature gradient which limits the amount of radiative losses by reducing the total gas mass in this region[2].

At higher temperature we see that the flow energy (FLOW) which incidentally consists primilarily of the termal energy of the gas and not of kinetic energy, dominates over the radiative contribution (see Fig. 4). This flow term increases slowly.

[2] If the radiative losses as indicated in Fig. 2 are overestimated, the steepness of the temperature gradient will be reduced.

© Springer-Verlag • Provided by the NASA Astrophysics Data System

1967ZA.....67..193U

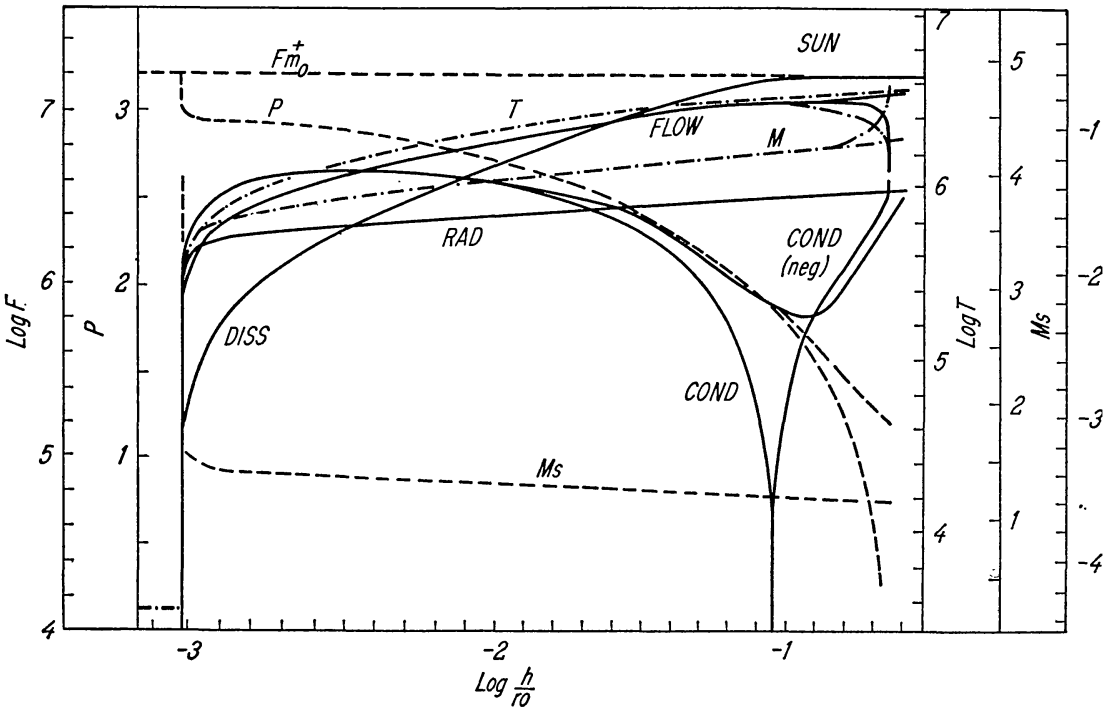

Fig. 4. Height dependence of various quantities above the point of shock formation in the solar model. P is the gas pressure, M_s the shock Mach number, T the temperature and M the flow Mach number. The quantities FLOW, RAD, COND, DISS represent energy fluxes (erg/cm²sec, scale F) integrated from the point of shock formation to the height level h. FLOW is the thermal and kinetic energy in the solar wind, RAD the radiation loss, COND the supply of energy by thermal conduction. DISS the supply of energy by shock dissipation. $\pi F_{m_0}^+$ is the total input of mechanical energy in form of noise (scale F) which ultimately becomes equal to DISS when at great heights all shock energy is dissipated. r_0 is the radius of the sun. At great heights the solutions show the splitting in super- and subcritical solutions. $\tilde{L} = 9$

Conduction finally becomes small compared with shock dissipation and vanishes with vanishing temperature gradient when the dissipated shock energy balances the sum of flow and radiated energies:

$$\text{DISS} = \text{FLOW} + \text{RAD} . \tag{6.4}$$

The influence of viscosity, which has been shown by SCARF and NOBLE, 1965, to be of importance in solar wind calculations, can be neglected in our models. The effect of viscosity being to u^2 and $u\frac{du}{dr}$ becomes important when the kinetic part of the flow energy FLOW dominates. This is not the case at lower heights, and at heights beyond 1.1 r_0 our models become unreliable at any rate because of the disparity of the supercritical and subcritical solutions.

© Springer-Verlag • Provided by the NASA Astrophysics Data System

1967ZA.....67..193U

2. Comparison with observations and with other models

a) Maximum coronal temperature T_{cor} and *electron density profile* Ne are compared with observations in the following Table and Fig. 5.

Table 4. *Maximum coronal temperature of our model compared with recent observations*

T_{cor} °K	Year	Author	Nature
$2 \cdot 10^6$	1965	CRONYN	radio-observation
$8 \cdot 10^5$	1964	KUNDU, DE JAGER	radio, x ray observation
$2.6 \cdot 10^6$	1963	BILLINGS LILLIEQUIST	line width observation
$1.5 \cdot 10^6$	1961	ELWERT	x ray observation
$3.2—3.5 \cdot 10^6$	1961	JARRETT, VON KLÜBER	line width observation
$2 \cdot 10^6$	1959	BILLINGS	line width observation
$3.2 \cdot 10^6$	1966	ULMSCHNEIDER	model

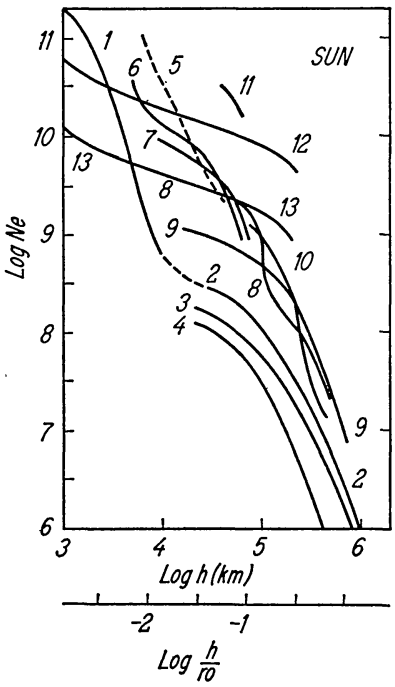

Fig. 5. Electron density Ne (cm^{-3}) is given as a function of height h (km) for the undisturbed solar atmosphere by (*1*) DE JAGER (1959), (*2*), (*3*), (*4*) VAN DE HULST (1953) and for the active region by (*5*) IVANOV-KHOLODNYI and NIKOLSKII (1961), (*6*) KAKINUMA and SWARUP (1962), (*7*) KAWABATA (1960), (*8*) CHRISTIANSEN et al. (1960), (*9*) NEWKIRK (1961), (*10*) HIEI (1962) and for a quiescent prominence by (*11*) KOELBLOED and KUPERUS (1963), (*12*) our non-viscous model, (*13*) our model including viscosity

b) The total ultraviolet flux πF_{RAD} in erg/cm² sec. has been estimated to be $2 \cdot 10^7$ (OSTERBROCK, 1961) and $2.5 \cdot 10^5$ (DE JAGER, 1959) which compares well with our result of $3.5 \cdot 10^6$.

c) The velocity of the solar wind flow u has been observed by BILLINGS and LILLIEQUIST, 1963, at $T = 1.03$ to be 6.6 km/sec which agrees fairly well with our 13.4 km/sec at this distance.

d) The solar mass flux $\varrho u r^2$ has been measured by Mariner II (NEUGEBAUER and SNYDER, 1962; COLEMAN et al. 1962) to be $8 \cdot 10^{-12}$ g/cm²sec. We find the much higher value of $9.9 \cdot 10^{-9}$. The following rough estimate shows however that the marine results seem too small. If we take the flow velocity observation of BILLINGS and LILLIEQUIST, 1963, and the observed electron densities (Fig. 5) at $r = 1.03$ we find for the mass flux $6 \cdot 10^{-10}$ to $1 \cdot 10^{-8}$ g/cm²sec. With this estimate our model value is in good agreement.

© Springer-Verlag • Provided by the NASA Astrophysics Data System

1967ZA....67..193U

e) The total mechanical flux input $\pi F^+_{m_0}$ in erg/cm²sec has been estimated to be $1 \cdot 10^6$ (SAITO, 1964), $1 \cdot 10^5$ (STURROCK, 1964), $3.3 \cdot 10^7$ (OSTERBROCK, 1961). Our value of $1.6 \cdot 10^7$ fits fairly well. A minimum estimate can be obtained by using the above estimate of the mass flux based on the observation of BILLINGS and LILLIEQUIST, 1963. The mere existence of supersonic flow and a coronal temperature of $2 \cdot 10^6$ °K gives with eq. (3.23) $5 \cdot 10^5 - 8.4 \cdot 10^6$ erg/cm²sec for the thermal and kinetic energy of the gas flow alone. An approximately equal amount of radiative flux has to be added to give an estimate for the mechanical flux input.

f) The steepness of the temperature rise may be compared with recent models. It turns out that our temperature rise is extremely steep due to the balance of the conduction and radiation. Almost all of these models do not include radiation and must lead therefore to less steep temperature gradients. The run through the temperature interval from $3 \cdot 10^4$ °K to $2 \cdot 10^5$ °K is given to be more than 200 km by UCHIDA, 1963, 48 km by KANNO and TOMINAGA, 1964, 100 km by ALLEN, 1965, as compared to 5.5 km by us. KUPERUS, 1965, gives a very steep gradient and ZIRIN and DIETZ, 1963, conclude from observations that there is a very steep temperature gradient.

VII. Discussion of the Stellar Results

Our stellar models behave very similarly to the solar model (see Figs. 6, 7, 8). Of course, non of the data could be checked against observations. A comparison will be given, however, with the available model calculation by KUPERUS, 1965.

1. The amount of convective noise energy produced by different stars

The amount of noise energy produced by a convection zone depends strongly on the value of the mean velocity $\bar{v}$ in the turbulent velocity field. For very hot stars ($T_e \geqq 15{,}000°$) and stars with very low surface gravity ($\log g \approx 1$) the inner ionization zone of hydrogen occurs already in the outer radiative equilibrium layer of the star and thus does not start a convection zone as is the case in cooler and more dense stars. With no convective motion no noise is produced by the processes considered in this paper.

It is readily seen from eq. (4.1) that the noise production is important only in a narrow region around the maximum of the velocity curve. Eq. (4.1) also limits the noise produced in the He-convection zones in very hot stars.

Noting that very close to the layer of maximum noise production, the total flux πF of the star is carried completely by convection, as is shown by VITENSE, 1953, (Fig. 5), we can understand the amount of noise

© Springer-Verlag • Provided by the NASA Astrophysics Data System

1967ZA.....67..193U

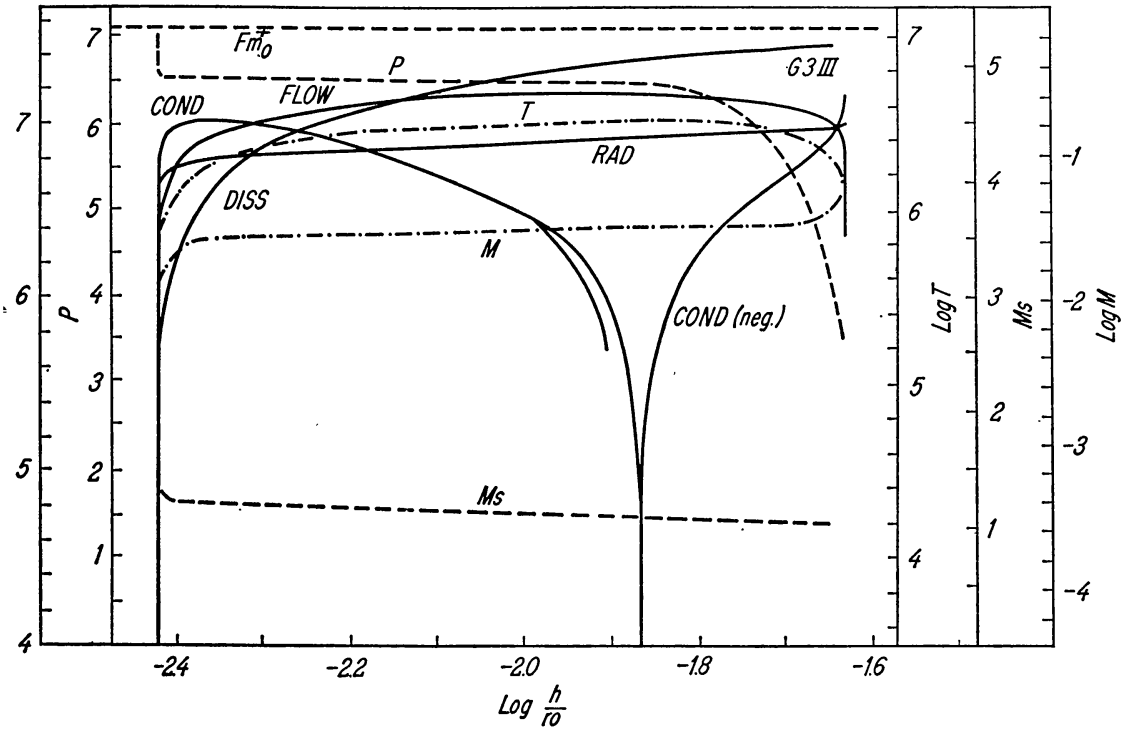

Fig. 6. Height dependence of various quantities above the point of shock formation in the model of a type G3 III star. Notation see Fig. 4

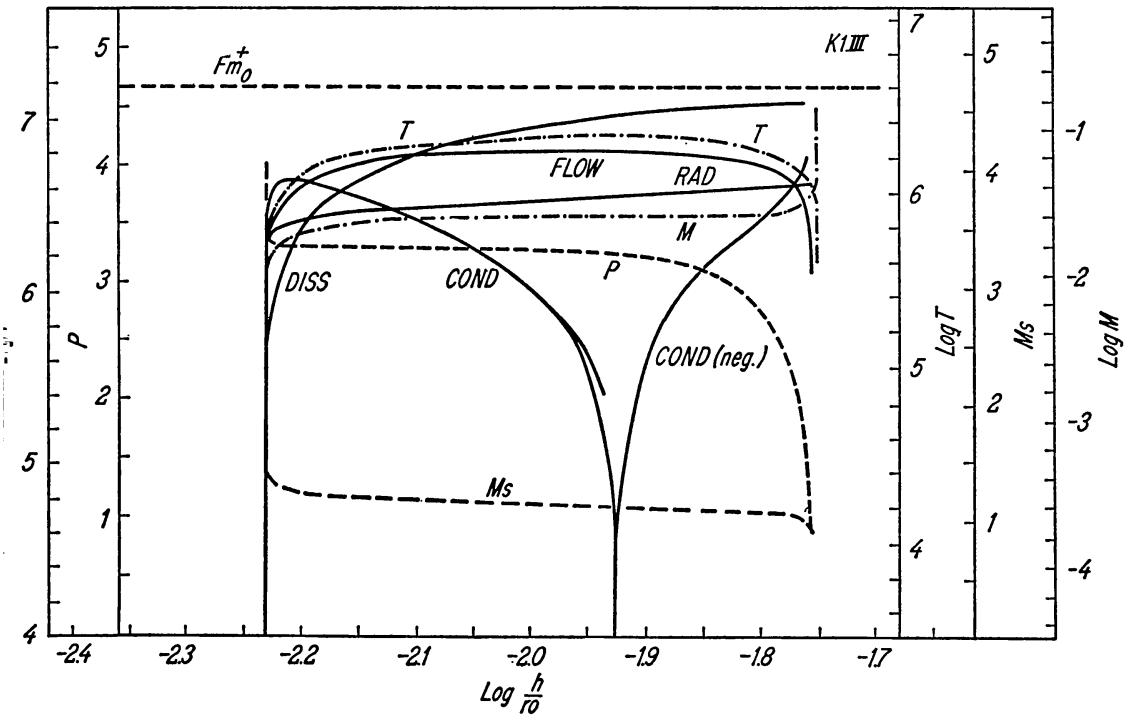

Fig. 7. Height dependence of various quantities above the point of shock formation in the model of a type K1 III star. Notation see Fig. 4

© Springer-Verlag • Provided by the NASA Astrophysics Data System

1967ZA.....67..193U

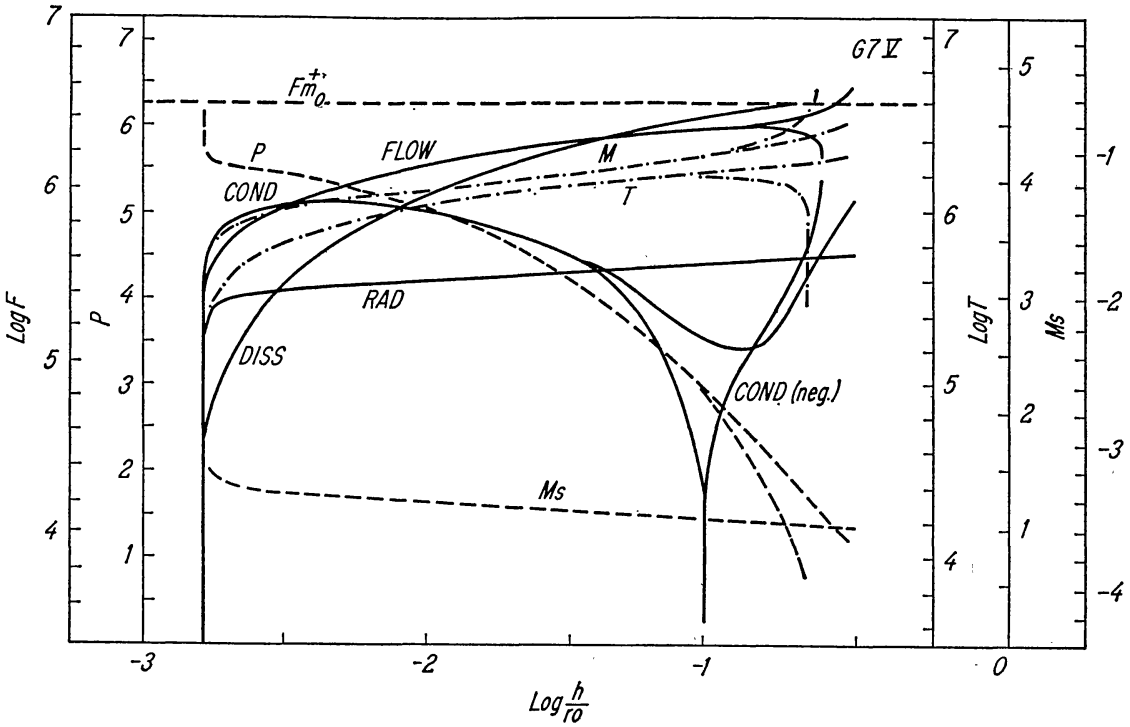

Fig. 8. Height dependence of various quantities above the point of shock formation in the model of a type G7 V star. Notation see Fig. 4

energy produced by a star as function of the effective temperature T_{eff} and the surface gravity as follows:

As the convective flux πF_k is proportional to $\bar{v}$ and the density ϱ, we can write for a point shortly before the velocity maximum $\bar{v}_{\max}$ is reached:

$$\sigma T_{\mathrm{eff}}^4 = \pi F = \pi F_K \sim \varrho \bar{v} \,. \tag{7.1}$$

From this equation one can deduce the following statement:

T 1: *The higher T_{eff} and the smaller g, the larger the noise energy production.*

This statement is valid only a convection zone of reasonable size can develop in a star, however, it is consistent with our models as well as those given by KUPERUS, 1965. A summary of our conclusions is given in Fig. 9.

2. *Coronal temperature and temperature gradients in the transition layers for different stars*

The height at which the shock is formed is determined entirely by the flux of noise energy and the scale height of the atmosphere. The temperature of the upper photosphere of the stars is roughly the same (3500 °K to 4500 °K). The less the noise flux and the lower the surface gravity the more extended the upper photosphere.

© Springer-Verlag • Provided by the NASA Astrophysics Data System

1967ZA.....67..193U

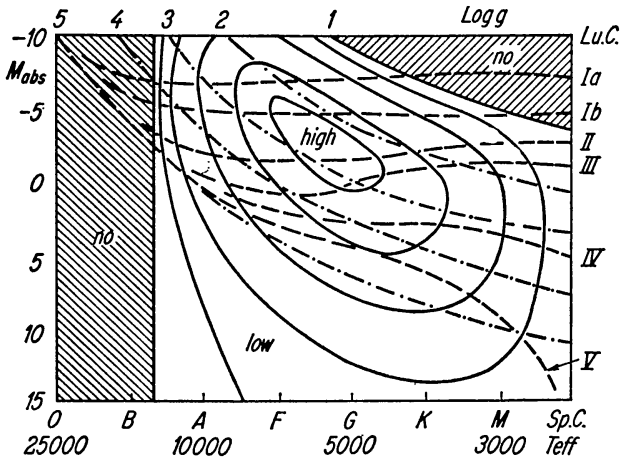

Fig. 9. Hertzsprung-Russel diagram with the qualitative lines of equal noise production. "high" labels regions of high, "low" regions of low and "no" regions of no noise production. These lines are also lines of equal ultraviolet radiation and mass fluxes as well as equal steepness of the temperature gradients in the transition layers and equal maximum coronal temperatures. Lines of equal Spectral class (Sp. C.) and equal surface gravities (g) are indicated

Most important for our considerations, however, is the pressure p_0 at the height of shock formation. Considering the similarity of boundary temperature T_0, and that this value enters eq. (4.7) only as $\sqrt{T_0}$, we can make the following statement, keeping this limitation in mind: (see Table 2).

T 2: *The pressures p_0 at the level of shock formation are proportional to the noise fluxes.*

T 3: *The ultraviolet radiative flux of a star is roughly proportional to the amount of noise energy produced.*

This can be ascertained in our models by comparing the „RAD"-profiles of our 4 stars (Figs. 4, 6, 7, 8) and correcting them by the factors p_0 (star)/p_0 (sun). All curves can be approximately made to coincide with the solar curve.

The lines of equal noise production in Fig. 9 are lines of equal $U - V$ fluxes.

Another important conclusion can be drawn from statements T2 and T3 by remembering that conduction (COND) is balancing the radiative losses (RAD) at the heights where most of the radiative losses occur. If the RAD-term is very large, the COND-term has to be very large and, consequently, the temperature gradient very steep. We can state therefore: (see Table 3).

T 4: *The steepness of the temperature gradient in the transition layer is roughly proportional to the amount ot noise produced.*

© Springer-Verlag • Provided by the NASA Astrophysics Data System

1967ZA....67..193U

However, the temperature gradient must be measured at temperatures above 10^4 °K because at lower temperatures the assumption COND = RAD is not valid as can be seen in Table 3. Again the lines of equal noise production in Fig. 9 are lines of equal steepness of the transition layer.

From Tables 1 and 2, invoking the similarity of the stellar boundary temperatures, keeping the limitations of this statement in mind, and using the equation

$$\text{mass flux} = \varrho_0 c_0 M_0 \tag{7.2}$$

where M_0 is the critical flow Mach number of the supersonic stellar wind flow, we find:

T 5: *The larger the noise flux the larger the mass flux due to stellar wind from the star.*

We then have that the lines of equal noise production in Fig. 9 are also lines of equal mass flux due to stellar winds.

Finally we deduce the following statement:

T 6: *The larger the noise flux the higher the coronal temperature of the star.*

The lines of equal noise flux in Fig. 9 are then lines of equal coronal temperatures. To prove this statement, we just note that, since a higher noise flux means higher mass flux, higher radiative losses, and steeper temperature gradients so that conduction may balance the radiative term, the temperature has already reached a higher value when the shock dissipation finally catches up with the FLOW and RAD terms.

3. *Comparison with* KUPERUS' *models*

The comparison with KUPERUS', 1965, models shows a general agreement in the behaviour of both the noise energies produced and the coronal temperatures. In addition our statements *T*. 1 and T. 6 agree very well with Table 9 in KUPERUS' paper.

The energy production is bigger by a factor 2 to 3, probably due to KUPERUS' more approximate method of computation.

The coronal temperatures are by a factor 3 to 4 lower which is probably due to the exhaustion of shock energy at greater heights because his theory depends on small shock Mach numbers and uses up more shock energy at lower heights in order to balance radiation.

I would like to thank Prof. Dr. LUDWIG OSTER for suggesting this investigation, and for continuous encouragement and helpful criticisms. The many discussions with Dr. JAMES HUNTER and Dr. N. PAUL PATTERSON are gratefully acknowledged. Financial support during the course of this work was provided by the Aerospace Research Laboratories of the Office of Aerospace Research, United States Air Force, Wright-Patterson AFB, Ohio. Funds for computer were provided by Yale University, and by the National Science Foundation through Yale University, and are gratefully acknowledged.

© Springer-Verlag • Provided by the NASA Astrophysics Data System

1967ZA....67..193U

References

Allen, C. W.: Astrophysical quantities. London: Athlone 1964.
— Space Sci. Rev. **4**, 91 (1965).
Aller, L. H.: Astrophysics. New York: Ronald 1963.
Billings, D. E.: Astrophys. J. **130**, 961 (1959).
—, and C. G. Lilliequist: Astrophys. J. **137**, 16 (1963).
Bird, G. A.: J. Fluid Mech. **11**, 180 (1961).
— Astrophys. J. **139**, 675 (1964); 684 (1964); **141**, 1455 (1965).
Böhm-Vitense, E.: Z. Astrophys. **46**, 108 (1958).
Brinkley, S. R., and J. G. Kirkwood: Phys. Rev. **71**, 606 (1947).
Chapman, S.: Smithsonian Contrib. Astrophys. **2**, 1 (1967).
Christiansen, W. N., D. S. Mathewson, J. L. Pawsey, S. F. Smerd, A. Boischot, J. F. Denisse, P. Simon, T. Kakinuma, H. Dodson-Prince, and J. Firor: Ann. Astrophys. **23**, 75 (1960).
Coleman, P. J., L. Davis, E. J. Smith, and C. P. Sonett: Science **138**, 1099 (1962).
Cronyn, W. M.: M. S. Thesis Univ. of Michigan, 1965.
Doherty, L. W., and D. H. Menzel: Astrophys. J. **141**, 251 (1965).
Elwert, G.: Z. Naturforsch. **7a**, 432 (1952).
— J. Geophys. Res. **66**, 391 (1961).
Heintze, J. R. W.: Rech. Ast. de l'obs., Utrecht **17**, (2) (1965).
Hiei, E.: J. Phys. Soc. Japan **17**, 227 (1962).
House, L. L.: Ap. J. Suppl. 8, 307 (1964).
Hulst, H. C. van de: The sun, ed. G. Kuiper. Chicago: University of Chicago Press 1953.
Ivanov Kholodnyi, G. S., and G. M. Nikolskii: Sov. Ast. **5**, 31 (1961).
Jager, C. de: Handbuch der Physik, Bd. 52, S. 80. Berlin-Göttingen-Heidelberg: Springer 1959.
— Res. in Geoph. **1**, 1 (1964) MIT Press, Cambridge, Mass.
Jarrett, A. H., and H. von Klüber: M. M. **122**, 223 (1961).
Kakinuma, T., and G. Swarup: Astrophys. J. **136**, 975 (1962).
Kanno, M., and S. Tominaga: Quoted by Pottasch (1964).
Kawabata, K.: Publ. Ast. Soc. Japan **12**, 513 (1960).
Koelbloed, D., and M. Kuperus: Proc. Kon. Ned. Ak. v. Wet. B **66**, 36 (1963).
Kundu, M. R.: Univ. Mich. Rad. Ast. Obs. Report Nr. 64-4 (1964).
Kuperus, M.: Rech. Ast. de l'Obs. d'Utrecht **17**, (1) (1965).
Landau, L. D., and E. M. Lifshitz: Fluid Mechanics, New York: Pergamon 1959.
Lüst, R.: Space Sci. Rev. **1**, 522 (1962).
Neugebauer, M., and C. W. Snyder: Science **138**, 1095 (1962).
Newkirk, G.: Astrophys. J. **133**, 983 (1961).
Oster, L.: Z. Astrophys. **44**, 26 (1957).
— Astrophys. J. **143**, 928 (1966).
Osterbrock, D. E.: Astrophys. J. **134**, 347 (1961).
Parker, E. N.: Interpl. Dyn. Proc. New York: Interscience 1963.
— Space Sci. Rev. **4**, 666 (1965).
— Astrophys. J. **141**, 1463 (1965).
Pottasch, S. R.: Space Sci. Rev. **3**, 816 (1964).
— B.A.N. **18**, 7 (1965).
Raju, P. K.: Ph. D. Thesis. Yale University 1966.
Saito, M.: Publ. Ast. Soc. Japan **16**, 179 (1964).
Scarf, F. L., and L. M. Noble: Astrophys. J. **141**, 1479 (1965).
Schatzmann, E.: Ann. Astrophys. **12**, 203 (1949).
Schirmer, H.: Z. Astrophys. **27**, 132 (1950).

© Springer-Verlag • Provided by the NASA Astrophysics Data System

1967ZA.....67..193U

Seaton, M. J.: Ann. Astrophys. **18**, 188 (1955).
Skalafuris, A. J.: Astrophys. J. **142**, 351 (1965).
Sturrock, P. A.: Nature **203**, 285 (1964).
Uchida, Y.: Publ. Ast. Soc. Japan **15**, 376 (1963).
Ulmschneider, P.: Ph. D. Thesis. Yale University 1966.
Vitense, E.: Z. Astrophys. **32**, 135 (1953).
Weymann, R.: Astrophys. J. **132**, 380 (1960).
— Astrophys. J. **132**, 452 (1960).
Whitaker, W. A.: Astrophys. J. **137**, 914 (1963).
Whitham, G. B.: J. Fluid Mech. **4**, 337 (1958).
Zirin, H., and R. D. Dietz: Astrophys. J. **138**, 664 (1963).
Zonnevield, J. A.: Autom. Num. Integr. Math. Centr., Amsterdam (1964).

Dr. Peter H. Ulmschneider
Astronomisches Institut
und Sternwarte der Universität
8700 Würzburg, Büttnerstraße 72

© Springer-Verlag • Provided by the NASA Astrophysics Data System